This study investigates the process of automated control over the operation of pumping stations along the main oil pipeline during start-up, stop, and pressure maintenance while oil pumping. Disturbances are considered as deterministic parametric variations of the coefficient of hydraulic resistance, which depend on changes in pressures, flows, including oil viscosity.

A control system has been designed that solves the problem of integrating recursive identification of model parameters with predictive formation of control effects in a single loop that covers start-up, operating mode, and compensation for disturbances. The main idea of automation is to transfer the functions of controlling the oil pipeline from pumping station operators to the dispatch center.

An adaptive-predictive control structure has been proposed that combines recursive identification of parameters, state assessment, and optimization predictive formation of control effects. The system integrates a Kalman filter for real-time state assessment and a module for recursive updating of model parameters. This provides online adaptation of the mathematical model of the facility without personnel intervention.

The application of the proposed approach reduces the accumulation of the integrated error in flow control under the operating mode by approximately 87 percent. After a viscosity jump, the flow does not go beyond the technological tolerance of ± 2 percent. The improvement in control quality is explained by the system's capability to predict the dynamics of the facility and compensate for uncertainties before their impact on the controlled variables. The algorithm automatically processes the full cycle: controlled start-up, entry into the operating mode, and maintaining pressures within the specified limits.

The results could be implemented in SCADA systems for oil pumping stations to be controlled from the dispatch center. This would increase the economic efficiency and stability of oil transportation modes

Keywords: Kalman filter, recursive identification, control over hydrodynamic modes, adaptive control, predictive control, mathematical model

UDC 681.5: 622.692.4
DOI: 10.15587/1729-4061.2026.359626

DESIGNING AN ADAPTIVE-PREDICTIVE SYSTEM TO CONTROL HYDRODYNAMIC MODES OF OIL TRANSPORTATION

Oleksandr Kuchmystenko
Corresponding author
Candidate of Technical Sciences*
E-mail: oleksandr.kuchmystenko@nung.edu.ua
ORCID: https://orcid.org/0000-0002-0457-7611
Mykhailo Shavranskyi
Candidate of Technical Sciences, Associate Professor*
ORCID: https://orcid.org/0009-0007-9858-9202
Yurii Puk
PhD Student*
ORCID: https://orcid.org/0009-0008-5297-1358
*Department of Automation and Computer-Integrated Technology
Ivano-Frankivsk National Technical University of Oil and Gas
Karpatska str., 15, Ivano-Frankivsk, Ukraine, 76019

Received 25.03.2026
Received in revised form 01.06.2026
Accepted date 10.06.2026
Published date 30.06.2026

How to Cite: *Kuchmystenko, O., Shavranskyi, M., Puk, Y. (2026). Designing an adaptive-predictive system to control hydrodynamic modes of oil transportation. Eastern-European Journal of Enterprise Technologies, 3 (2 (141)), 139–152. https://doi.org/10.15587/1729-4061.2026.359626*

1. Introduction

The current stage of development of the oil and gas industry is characterized by increasing requirements for the efficiency and reliability of transport systems, which is due to both economic factors and the need to ensure uninterrupted supply of oil to processing plants. Main oil pumping stations (MPSs) are a key link in the oil pipeline transport system. The operating modes of MPSs directly determine the energy consumption, productivity, and reliability of the oil transportation system as a whole. The task of optimal control over the hydrodynamic modes of MPSs remains open due to the variability in the physical and chemical properties of oil and the incompleteness of information about disturbing factors.

In industrial practice, MPS control is mainly implemented on the basis of PID controllers and deterministic models of hydraulic processes. This approach has limited effectiveness under non-stationary modes and in the presence of significant disturbances – that is, precisely under the conditions that dominate operation. Among the main complicating factors are temperature-dependent changes in oil viscosity, uneven product supply from different suppliers, as well as gradual degradation of equipment characteristics. Devising adaptive and optimal control methods, together with the growth in computing capabilities, creates prerequisites for building control systems that maintain the quality of control under variable operating conditions and incomplete information about the object.

A promising direction is the integration of adaptive schemes with predictive control (Model Predictive Control, MPC), which makes it possible to take into account the dynamics of the object on the forecast horizon and simultaneously react to changes in its parameters in real time.

Therefore, it is a relevant task, both from scientific-theoretical and practical points of view, to design adaptive-predictive control systems for hydrodynamic regimes of main oil pipelines with the integration of recursive identification and predictive control methods.

2. Literature review and problem statement

The task of adaptive-predictive control over hydrodynamic modes of oil pumping systems is at the intersection

of several scientific areas: hydraulics of pipeline systems, automatic control theory, identification of dynamic objects, and intelligent computing technologies. Despite the significant amount of accumulated knowledge in each of these areas, their system integration with respect to the tasks of controlling the modes of main oil pipelines with pumping stations and tank farms remains insufficiently studied.

Hydraulic modeling of pipeline systems is traditionally based on the equations of conservation of mass and momentum in a one-dimensional statement. For non-stationary modes, the classical approach is the method of characteristics, developed in detail in [1]. However, it is focused on the analysis of fast wave processes and is excessively expensive for the synthesis of real-time control. The issue of constructing simplified models for regulators is not considered in [1]. In [2], explicit approximations of the Colebrook-White equation for the friction coefficient λ are systematized. At the same time, the accuracy of these approximations is estimated only for stationary flow regimes. Their behavior under rapid changes in viscosity is not investigated. In [3], the acceptability of lumped models with spatial discretization for real-time problems is shown. However, the model in [3] is built for gas flows with constant medium properties. The transfer of the approach to oil pipelines with variable viscosity is not justified. The reason is that papers [1–3] lack a mechanism for online refinement of the hydraulic parameters of the simplified model.

Identification of parameters for hydraulic systems under conditions of variable rheological properties of oil is a separate urgent task. In [4], it is shown that the kinematic viscosity of oil varies from $3 \cdot 10^{-6}$ to more than $8 \cdot 10^{-6}$ m^2/s. However, study [4] is limited to hydraulic calculations and does not consider the consequences of variability for control loops. In [5], accurate explicit approximations of the friction coefficient in a wide range of Reynolds numbers are proposed. At the same time, in [5], the approximation error is not related to the quality of the closed-loop control. In [6], the theory of the Kalman filter for state estimation under noise conditions is systematized. In [7], filtering algorithms with restrictions on the state vector are generalized. However, the objects in [6, 7] are abstract dynamical systems. The specificity of hydraulic objects with parametric disturbances from viscosity is not taken into account in these papers. The reason is the lack of connection between the disturbance model and the physics of friction.

Classical PID control remains the most common approach in industrial automation of pumping stations. In [8], an overview of tuning methods and limitations of PID controllers is presented; the fundamental impossibility of explicitly taking into account technological constraints within the framework of the classical approach is indicated. For long pipeline systems with significant transport delay, this leads to a systematic violation of pressure constraints in transient regimes.

Model predictive control (MPC) has become widely used due to its ability to explicitly take into account constraints in the optimization problem. In [9], a linear implementation of MPC in the form of increments is given, convenient for practical implementation. A feature of [9] is that the object model is considered to be precisely known and unchanging. In [10], an overview of industrial MPC technologies is performed and their advantages for multidimensional objects are shown. At the same time, in [10] it is stated that most implementations work with fixed models. The mechanisms of adaptation to parameter drift are not analyzed in [10]. Work [11] lays the theoretical foundation for the stability of MPC with constraints, and its peculiarity is that the results were obtained assuming an exact model without parametric disturbances. In [12], non-stationary hydraulic processes were modeled taking into account pressure constraints but there is no coordination of several consecutive pumping stations by a single optimization loop. The common reason is the gap between the MPC theory and the variable hydraulics of a real oil pipeline.

The class of adaptive-predictive systems is formed by combining MPC with adaptive identification. In [13], methods of nonlinear predictive control with online model updating are systematized; however, the algorithms considered are computationally complex for typical pumping station controllers. In [14], delayed and irregular measurements in the extended Kalman filter are taken into account, and it is focused on chemical reactors and does not concern distributed hydraulic objects. In [15], the foundations of recursive identification of dynamic systems are laid but, at the same time, the problem of loss of excitation in well-stabilized loops is not solved. In [16], the stability of a closed loop with a limited adaptation rate is investigated, but the conditions are formulated for general models without taking into account technological pressure constraints.

The pumping equipment at oil pumping stations is described by the quadratic pressure-flow characteristic $H = a_0 n^2 - a_1 Q^2$, which is well studied and given in the fundamental treatise [17]. Controlling the speed of pumps with simultaneous limitation of the output pressure requires solving an optimization problem with constraints in the form of permissible ranges, which goes beyond the limits of classical PID control. In [9] it is shown that problems of this class are a typical example of the application of the MPC approach.

The use of intelligent technologies for the identification and control of hydraulic objects is a promising direction. In [18] it is shown that a hybrid approach that combines machine learning with a physical model significantly exceeds purely data-oriented and physical models in terms of flow estimation accuracy. In [19], a theoretical basis for nonlinear system identification using neural networks and fuzzy models was developed, which can be used to improve the hydraulic model of the pipeline.

Our review of the literature [1–19] shows that individual components of the problem have already been worked out in detail and there are hydraulic models of pipeline systems, methods of state assessment, adaptive identification, and model-predictive control. But at the same time, the task of coordinated control over multi-section oil pipelines with variable rheological properties of the transported product and ensuring pressure constraints along the entire route within a single algorithm remains unsolved. This can be explained by the need to simultaneously take into account spatially distributed hydrodynamics, parametric uncertainty, and technological constraints in real time.

Papers [1–3] lack a mechanism for online refinement of the parameters of simplified hydraulic models. In [4–7], state estimation is not related to the physical nature of parametric disturbances caused by viscosity changes. Therefore, the task of integrating adaptive identification, state estimation, and predictive optimization within a single control loop for the entire operating cycle of the oil pipeline remains unsolved. In [8], the fundamental impossibility of explicitly taking into account constraints by the classical PID approach is

proven. In [9–12], predictive control is based on fixed models without coordination of several stations. In [13–16], adaptive extensions are not brought to the level of hydraulic objects with pressure constraints. The integration of recursive identification of model parameters with predictive formation of control influences in a single control loop covering start-up, operating mode, and compensation of viscosity disturbances remains insufficiently studied. One possible approach to solving this task is to combine adaptive identification based on the Kalman filter with model-predictive control within a single closed system. This is the approach used in our work for a main oil pipeline, in which a change in the rheological properties of the transported product is considered as a parametric perturbation of the model.

This allows us to argue that it is advisable to conduct a study aimed at designing an adaptive-predictive control system for a main oil pipeline taking into account variable hydrodynamic parameters and technological constraints.

3. The aim and objectives of the study

The purpose of our study is to design an adaptive-predictive control system for the hydrodynamic modes of a conditional pipeline under conditions of parametric uncertainty. This will make it possible to automatically compensate for changes in oil viscosity without stopping pumping and manually reconfiguring regulators. In addition, this will reduce the risk of violating technological pressure restrictions along the route.

To achieve the goal, the following tasks were set:

– to construct a mathematical model of hydrodynamic processes along a section of the main oil pipeline taking into account parametric uncertainty and variable oil characteristics;

– to synthesize an adaptive-predictive regulator for controlling oil transportation modes taking into account technological restrictions;

– to assess the state and perform recursive identification of the parameters of the hydrodynamic system under conditions of measurement noise;

– to synthesize predictive control with compensation for unmeasured disturbances and adaptive identification of parameters;

– to investigate the effectiveness of the integrated control system in the MATLAB environment (USA) under different operating modes of the main oil pipeline.

4. The study materials and methods

The object of our study is the process of automated control over the operation of pumping stations along the main oil pipeline at start-up, stop, and pressure maintenance during oil pumping.

The principal hypothesis assumes that the combination of the assessment of unmeasured disturbance by the Kalman filter with predictive optimization makes it possible to keep the flow rate within the technological tolerance of ± 2% with a sudden change in pressure, flow rate, or viscosity of oil. In this case, the quality of control will be significantly higher than that of a classical PID controller with fixed settings.

The following assumptions were adopted. The oil flow is considered single-phase, isothermal, and turbulent over the entire range of studied modes. Viscosity affects the hydraulic resistance – its variations are interpreted as parametric perturbations of coefficient K_h. Measurement errors are approximated by Gaussian noise with known covariances, which corresponds to flowmeters of accuracy class ± 0.5%. The pressure characteristics of the pumps are given by the specifications and are considered unchanged.

The following simplifications were accepted. The hydrodynamics problem is considered in a one-dimensional statement with a quasi-stationary approximation for the friction coefficient. Wave processes are neglected since the wave propagation time ($L / c \approx 167$ s) is much less than the characteristic time of technological disturbances. The route profile is given by a sinusoidal dependence as a test geodetic scenario, and not by the real terrain. Both pumping stations are assumed to be identical in characteristics. For the synthesis of the controller, the distributed model is reduced to a lumped first-order one and linearized in the vicinity of the operating point $Q0 = 0.55$ m^3/s. Deviations from the operating point are compensated by adapting the model in real time.

The object of the study is a spatially distributed hydrodynamic system with two pumping stations. NPS-1 is located at the beginning of the route ($x = 0$), NPS-2 – at a distance of 100 km; the pipeline ends with a tank farm at $x = L = 200$ km. Two active stations together with an extended hydraulic section between them form a control object with distributed parameters.

The control object is a main oil pipeline with a length of $L = 200$ km, which operated under conditions of variable hydrodynamic regimes. The geometric parameters of the pipeline were set by the internal diameter $D = 720$ mm and the wall thickness $\delta = 12$ mm. The pipe material is carbon steel, grade 17G1S, characterized by absolute roughness $\varepsilon = 0.046$ mm. These parameters determined the level of hydraulic resistance and pressure loss during transportation.

Physical properties of the working medium: crude oil with a density of $\rho = 870$ kg/m^3, kinematic viscosity is $4 \cdot 10^{-6}$ m^2/s at a temperature of 20°C. The viscosity value determines the flow regime and, accordingly, the coefficient of hydraulic friction, which is taken into account when building the model.

Nominal flow rate – $Q_{sp} = 0.55$ m^3/s (1980 m$_3$/h). Each station is equipped with four centrifugal pumps NM 3600–230; under nominal mode , one unit develops a pressure of $\Delta P = 3.5$ MPa (35 bar), which is sufficient to compensate for friction losses and geodetic lift.

The final section is completed by a tank farm of four RVS-20000 tanks. Back pressure – $P_{tank} = 1.5$ bar; this is the limit value at the outlet of the pipeline.

The route profile is given by dependence

$$z(x) = 20 \cdot \sin\left(\frac{\pi x}{L}\right) + 5 \cdot \sin\left(\frac{2\pi x}{L}\right).$$

The maximum height is 25 m. Such a height distribution formed a variable hydrostatic component of pressure along the pipeline. This complicated the flow dynamics and needed to be taken into account in the predictive model.

Technological constraints determine the permissible area of system operation and are used during the synthesis of control algorithms. They apply to both distributed variables (pressure along the route) and concentrated ones (flow rate and pump speeds).

The pressure at any point in the pipeline must remain within the permissible interval given by inequality (1)

$$P_{\min}=2.0\ \text{bar}\le P(x,t)\le P_{\max}=40\ \text{bar},\forall x\in[0,L]. \quad (1)$$

The lower limit corresponds to the condition of cavitation-free operation of pumps, and the upper limit limits mechanical stresses in the pipeline. For NPS-2, the condition $PS2_{in} \geq 8$ bar is additionally accepted, which ensures the permissible operating mode of pumping units.

The main controlled variable is the flow rate Q, the permissible range of which is determined by inequality (2)

$$0.4\frac{\text{m}^3}{\text{s}}\le Q(t)\le 1.2\frac{\text{m}^3}{\text{s}}. \quad (2)$$

The flow rate limits are selected taking into account the characteristics of the pumping equipment and transportation conditions; these same limits are used when building a predictive model and calculating control effects.

The maximum head of pumping stations is limited by condition (3)

$$\Delta P_{\text{pump}}\le 3.5\ \text{MPa}\left(\text{nominal head of NPS}\right), \quad (3)$$

which corresponds to the nominal operating mode of the pumping units. Exceeding this value is considered as equipment overload.

The operation of the facility was considered under several characteristic modes, which differ in process dynamics and control requirements. The initial stage of operation corresponded to the pressurization mode, within which the pipeline was gradually filled and the pressure increased from zero to the operating level. The pumping units were brought to the specified mode according to a linear law, which ensured the predictable dynamics of the system. Under this mode, the rate of pressure change was limited, which should not exceed 0.5 bar/s, since exceeding this value could lead to water hammer and damage to the equipment.

The second is a stationary mode maintaining the flow rate $Q = Q_{sp}$ with an accuracy of ± 2% (± 11 l/s) with minimal operator intervention.

The third is a transitional mode. It occurs when the physicochemical properties of oil or temperature conditions change. The control system must compensate for disturbances without exceeding the constraints (1) to (3), which necessitates an adaptive-predictive approach.

5. Research results and synthesis of an adaptive-predictive controller

5. 1. Mathematical modeling of oil pipeline hydrodynamics with parametric uncertainty

The mathematical model of the main oil pipeline hydrodynamics is based on a system of continuity and momentum equations describing the unsteady motion of a compressible fluid in the pipeline network. This approach makes it possible to take into account the spatiotemporal variation of hydraulic parameters and the nonlinear nature of energy losses [1].

The mass and momentum conservation equations take the form:

$$\frac{\partial\rho}{\partial t}+\frac{\rho}{A}\cdot\frac{\partial Q}{\partial x}=0, \quad (4)$$

$$\frac{\partial Q}{\partial t}+\frac{A}{\rho}\cdot\frac{\partial P}{\partial x}+\frac{\lambda}{2DA^2}\cdot Q|Q|+g\cdot A\cdot\frac{\partial z}{\partial x}=0. \quad (5)$$

In the above relations, $Q(x, t)$ determines the volumetric flow rate, $P(x, t)$ is the pressure distribution along the pipeline, $A = \pi D^2 / 4$ is the cross-sectional area, λ is the Darcy-Weisbach hydraulic friction coefficient, D is the internal diameter of the pipeline, $z(x)$ is the geometric profile of the route. Equation (4) reflects the mass balance, while (5) describes the momentum dynamics taking into account dissipative losses and the gravitational component.

The hydraulic resistance to flow is determined through the Colebrook-White equation, which is implicit in relation to the friction coefficient

$$\frac{1}{\sqrt{\lambda}}=-2\cdot\log_{10}\left(\frac{\varepsilon}{3.7D}+\frac{2.51}{Re\cdot\sqrt{\lambda}}\right),\quad Re=\frac{QD}{A\nu}. \quad (6)$$

For the numerical start, an explicit approximation (Swamee-Jain initial approximation) is used

$$\lambda_0=\frac{0.25}{\left[\log_{10}\left(\frac{\varepsilon}{3.7D}+\frac{5.74}{Re^{0.9}}\right)\right]^2}. \quad (7)$$

Under nominal flow conditions, the Reynolds number is $Re \approx 2.4 \cdot 10^5$ (at operating flow rate $Q_0 = 0.55 \text{m}^3/\text{s}$), which corresponds to a fully turbulent regime. The obtained value of the coefficient $\lambda \approx 0.0156$ is ensured after 5–7 iterations of numerical refinement with the convergence criterion $\varepsilon_\lambda < 10^{-6}$.

In the stationary approximation, when local inertial effects are insignificant, the system reduces to a first-order differential equation [1, 3]

$$\frac{dP}{dx}=-\rho g\cdot\frac{dz}{dx}-K_h\cdot Q|Q|,\quad K_h=\frac{\lambda\rho}{2DA^2}. \quad (8)$$

Discretization of the spatial domain is carried out by the method of backward integration from the end of the pipeline to its beginning with a step of $\Delta x = 1$ km

$$P_i=P_{\{i+1\}}+K_h\cdot\Delta x\cdot Q|Q|+\rho g\cdot\left(z_{\{i+1\}}-z_i\right),i=N,\ldots,1. \quad (9)$$

The boundary condition was set to the pressure in the tank farm $P(L) = P_{tank} = 1.5$ bar. At the location of NPS-2, an additional pressure jump $\Delta P_{\text{NPS},2}$ was taken into account, after which the integration continued in the direction of NPS-1. This scheme allowed us to restore the full spatial distribution of $P(x)$ along the route.

Local pressures at the pumping stations are determined through the value of the distributed field

$$P_{\text{NPS}_{in},k}=P\left(x_k\right),\quad P_{\text{NPS}_{out},k}=P_{\text{NPS}_{in},k}+\rho\cdot g\cdot H\left(Q,\bar{n}_k\right), \quad (10)$$

where the pump characteristic is given by the following dependence

$$H\left(Q,\bar{n}\right)=a_0\cdot\bar{n}^2-a_1\cdot Q^2.$$

The calibration of the parameters is carried out according to the passport point of the head characteristic, at $\bar{n}=1$ and $Q = 0.85\ \text{m}^3/\text{s}$, each pumping station provides a pressure of $\Delta P = 3.5$ MPa (the operating point of transportation in this case corresponds to $Q0 = 0.55\ \text{m}^3/\text{s}$, $\bar{n}_0=0.9285$)

$$a_0 = 554.5 \text{ m}, \quad a_1 = 200 \text{ m} \cdot \frac{\text{s}^2}{\text{m}^6}. \tag{11}$$

The consistency check is performed by substituting the input data into formula $\Delta P = \rho g \cdot (a_0 - a_1 \cdot Q^2)$. For the passport point ($\overline{n} = 1$; $Q = 0{,}85$ м^3/с) $\Delta P \approx 3.50$ MPa is obtained. This confirms the fulfillment of the energy balance of the pumping station model.

To describe the integrated dynamics of the flow rate, a nonlinear differential equation is used

$$\left(\frac{\rho L}{A}\right) \cdot \frac{dQ}{dt} = \Delta P_{\text{NPS},1} + \Delta P_{\text{NPS},2} - \\ - Kh \cdot L \cdot Q|Q| - \rho g \cdot \Delta z - \Delta P_{in}. \tag{12}$$

This equation determines the inertial properties of the system and is the basis for the synthesis of control algorithms since it describes the balance between the driving head and losses.

The transition from the distributed model (4), (5) to the concentrated model (12) is justified as follows. The characteristic time of changing the settings and technological disturbances (minutes–tens of minutes) significantly exceeds the propagation time of the acoustic wave along the route ($L / c \approx 167$ s); therefore, wave processes in the flow control problem can be neglected, and the spatial flow gradients can be considered small: $Q(x, t) \approx Q(t)$ along the entire route. A similar approach was used in [3] for real-time pipeline systems. NPS-1 and NPS-2 are taken into account through the total head $Q(x, t) \approx Q(t)$, which is determined from equations (10), (11). Deviations in the pump unit speeds from the rated values form a control vector $u = \left[\Delta\overline{n}_1, \Delta\overline{n}_2\right]^T$ in the state space (20), (21).

The initial conditions of the pressing phase correspond to the atmospheric pressure level

$$P(x, t=0) = P_{atm} = 1.0 \cdot 10^5 \text{ Pa} \approx 1 \text{ bar}. \tag{13}$$

The pump speed increases according to a linear law

$$\overline{n}(t) = \overline{n}_{\max} \cdot \frac{t}{T_{pres}} = 0.9 \cdot \frac{t}{1800}, \quad t \in \left[0, T_{pres}\right]. \tag{14}$$

The pressure field calculation is performed at a time step $\Delta t = 2$ s using the discrete model (9). To ensure physical correctness, during the pressing phase, a constraint is introduced

$$P(x, t) \geq P_{atm}. \tag{15}$$

This excludes the occurrence of unphysical absolute pressure values and ensures the stability of the numerical solution.

5. 2. Synthesis of an adaptive-predictive oil transportation controller taking into account technological constraints

The synthesis of an adaptive-predictive controller is based on the linearization of a nonlinear model of the pipeline system near the operating point corresponding to the nominal transportation mode. This approach allows us to move from a nonlinear description to a locally equivalent linear model suitable for building predictive control.

The linearization of dynamics equation (12) is performed near the operating point of the stationary mode ($Q0$, $\overline{n}_0$). Deviations are introduced

$$\Delta Q = Q - Q_0, \quad \Delta\overline{n} = \overline{n} - \overline{n}_0. \tag{16}$$

The result is a linear model in the following form

$$T_{ob} \cdot \frac{d\Delta Q}{dt} = K_{ob} \cdot \left(\Delta\overline{n}_1 + \Delta\overline{n}_2\right) - \Delta Q, \text{'} \tag{17}$$

where the object parameters are defined as:

$$T_{ob} = \frac{\rho L}{A \cdot B_q}, \quad K_{ob} = \frac{B_n}{B_q}, \tag{18}$$

and additionally:

$$B_n = 2\rho g \cdot a_0 \cdot \overline{n}_0, \quad B_q = 4\rho g \cdot a_1 \cdot Q_0 + 4K_h \cdot L \cdot |Q_0|. \tag{19}$$

At nominal values $Q0 = 0.55$ m^3/s and $\overline{n}_0 = 0.9285$ model parameters take the values $T_{ob} \approx 14.8$ s and $K_{ob} \approx 0.305$, which characterizes the inertia of the system and the degree of influence of the control actions of the pumping units.

The transfer function of the linearized model takes the form

$$W(s) = \frac{K_{ob}}{T_{ob} \cdot s + 1}.$$

For discrete representation, a state space model is used:

$$x(k+1) = A_d \cdot x(k) + B_d \cdot u(k) + w(k), \tag{20}$$

$$y(k) = C_d \cdot x(k) + v(k). \tag{21}$$

Discretization of the linearized model (17) at a step $\Delta t = 2$ s gives parameters $a = \exp(-\Delta t / T_{ob}) \approx 0.874$ and $b = K_{ob} \cdot (1 - a) \approx 0.039$ (the influence of one pump unit). Although model (12) is first order in terms of flow, the state vector is assumed to be two-dimensional: $x(k) = [\Delta Q(k); d(k)]^T \in R^2$, where $\Delta Q(k) = Q(k) - Q_{sp}$ is the flow deviation from the setpoint, and $d(k)$ is an unmeasured equivalent flow disturbance generated by parametric variations of the coefficient K_h due to changes in viscosity; its dynamics are modeled by a random walk $d(k + 1) = d(k) + wd(k)$. The expansion of the state vector by the disturbance state is a standard offset-free MPC (disturbance observer) technique [21]. The control vector is the absolute deviation in the pump speeds from rated $d(k + 1) = d(k) + wd(k)$. Accordingly, the matrices of system (20), (21) take the form: $A_d = [a\ 1; 0\ 1] \in R^{2\times2}$, $B_d = [b\ b; 0\ 0] \in R^{2\times2}$, $C_d = [1\ 0] \in R^{1\times2}$; $w(k)$ and $v(k)$ are Gaussian process noise and measurement noise, respectively. Thus, the first line A_d reproduces the discrete dynamics of the first order flow, the second is the disturbance model; the Kalman filter (22) to (25) estimates both state coordinates simultaneously.

5. 3. State estimation and recursive identification of hydrodynamic system parameters under measurement noise

State estimation is performed based on the discrete Kalman filter, which implements a recursive prediction and correction procedure [6].

The prediction stage is described by the following equation

$$\hat{x}(k|k-1) = A_d \cdot \hat{x}(k-1|k-1) + B_d \cdot u(k-1). \tag{22}$$

The covariance matrix is updated according to the process and measurement noise statistics. The Kalman gain is defined as

$$K_k = P_{k|k-1} \cdot C_d^T \cdot \left[C_d \cdot P_{k|k-1} \cdot C_d^T + R_v \right]^{-1}. \quad (23)$$

The status update was performed according to the following rule

$$\hat{x}_{k|k} = \hat{x}_{k|k-1} + K_k \cdot \left[y(k) - C_d \cdot \hat{x}_{k|k-1} \right]. \quad (24)$$

The update of the error covariance matrix takes the following form

$$P_{k|k} = \left(I - K_k \cdot C_d \right) \cdot P_{k|k-1}. \quad (25)$$

This structure provides an optimal state estimate in the sense of minimizing the root-mean-square error under Gaussian noise conditions. The assumption about a normal distribution is standard for the linear Kalman filter [6]. It is justified for flowmeters of accuracy class ± 0.5%, the errors of which are approximated by a normal distribution. Two types of disturbances are taken into account in our work. The first is parametric variations of coefficient K_h, which are tracked by the disturbance state $\hat{d}$ (fast compensation channel) and recursive identification of the dynamics parameter (28) to (29) (slow model refinement channel). The second is the measurement noise $v(k)$, filtered by the Kalman filter (22) to (25). The noise covariances are given as $Q_f = \text{diag}(10^{-6}, 10^{-7})$ and $R_f = 2.5 \cdot 10^{-5}$ (m^3/s)^2. The Q_f matrix has a dimension of 2×2, consistent with the dimensionality of state vector $x \in R^2$: the first diagonal element corresponds to the process noise in the flow rate, the second to the intensity of the random walk of disturbance d. The R_f scalar corresponds to the root-mean-square noise of 0.005 m^3/s of a flow meter of accuracy class ±0.5%. The notations Q_f and R_f are used to avoid collision with the weighting coefficients Q_w, R_w of functional (26) and the flow symbol Q. In addition to filtering the measurement noise, the filter simultaneously forms an estimate of the unmeasured disturbance, the dynamics of which are shown in Fig. 8.

5. 4. Synthesis of predictive control with compensation of unmeasured disturbances and adaptive parameter identification

Predictive control is formalized through optimization of the quadratic quality functional

$$J = \sum_{i=1}^{H_p} \left[\left\| y(k+i|k) - y_{sp} \right\|_{Qw}^2 + \left\| \Delta u(k+i-1) \right\|_{Rw}^2 \right], \quad (26)$$

where the first sum is taken over the forecast horizon $i = 1, \ldots, H_p$, and the control increments $\Delta u(k + i - 1)$ are non-zero only at the control horizon, i.e., for $i \le H_u$ (for $i > H_u$ $\Delta u = 0$ is taken); Q_w and R_w are the penalty weights for output deviation and control intensity, respectively. The optimization problem is stated taking into account technological constraints

$$0.5 \le \bar{n}_k \le 1.1, \quad \left| \Delta \bar{n}_k \right| \le 0.02, \quad P_{\min} \le P(x,k) \le P_{\max}. \quad (27)$$

The tuning parameters are taken to be $H_p = 10$ steps (corresponding to 20 s), $H_u = 3$ steps, weighting factors $Q_w = 100$ and $R_w = 50$. As a result, the problem is reduced to quadratic programming: $\min \frac{1}{2} \cdot \Delta U^T \cdot H \cdot \Delta U + f^T \cdot \Delta U$ at constraints $G \cdot \Delta U \le h$ [20]. The analytical solution to the problem for the first step of the sliding horizon takes the form

$$\Delta u^*(k) = -K_x \cdot \Delta \hat{Q}(k) - K_f \cdot \left(\hat{d}(k) + b \cdot \bar{u}(k) \right),$$

where $\bar{u}(k) = \Delta \bar{n}_1(k) + \Delta \bar{n}_2(k)$ is the total deviation in the pump speeds from rated; for the nominal parameters of the model $K_x \approx 0.64$, $K_f \approx 6.03$. By including the disturbance estimate $\hat{d}$ in the free component of the forecast, the control compensates for the parametric uncertainty before its manifestation in the controlled variable, which corresponds to the offset-free MPC structure [21].

Adaptive RMNK-identification of the model parameters is performed using the recursive least squares method with a forgetting factor. The parameter vector update is described by the following equation

$$\hat{\theta}(k) = \hat{\theta}(k-1) + L(k) \cdot \left[y(k) - \varphi^T(k) \cdot \hat{\theta}(k-1) \right]. \quad (28)$$

The algorithm gain is defined as

$$L(k) = \frac{P(k-1)\varphi \cdot (k)}{\lambda_f + \varphi^T(k) \cdot P(k-1) \cdot \varphi(k)}, \quad \lambda_f = 0.995, \quad (29)$$

where $\lambda_f = 0.995$ sets the exponential decay of information and corresponds to an effective memory window of about 200 discrete steps. The dynamics parameter a is subject to identification, determined by the hydraulic resistance and therefore varies with the viscosity of the oil; the transmission coefficient b is registered according to the pump pressure characteristic, since with an almost constant control signal under the quasi-stationary mode, separate identification of b and the steady disturbance is impossible (the regressors are collinear). To protect against estimate bias and covariance windup under the steady mode, the update is performed only with sufficient excitation $\left| \Delta \hat{Q}(k-1) \right| > 4 \cdot 10^{-3}$ m^3/s, , while the regression target is cleared of the disturbance estimate $\hat{d}$, which allows the model to be refined in real time without violating the stability of the closed loop.

The effectiveness of the synthesized adaptive-predictive controller is evaluated by integrated and temporal quality criteria that characterize the dynamics of the system under transient and quasi-stationary regimes. The control error is defined as the deviation in the controlled variable from the set flow value:

$$\text{IAE} = \int_0^T \left| e(t) \right| \text{d}t, \quad e(t) = Q(t) - Q_{sp}, \quad (30)$$

$$\text{ISE} = \int_0^T e2(t) \text{d}t, \quad (31)$$

$$\text{ITAE} = \int_0^T t \cdot \left| e(t) \right| \text{d}t. \quad (32)$$

The IAE criterion (Integrated of absolute error) characterizes the total deviation in the output variable from the given mode and is used as a generalized measure of control accuracy. The ISE criterion (Integrated of squared error) reacts more strongly to large deviations; therefore, it is more sensitive to emergency modes and sharp disturbances. The ITAE criterion (Integrated of time-weighted absolute error) takes into account not only the magnitude but also the duration of the error, which makes it possible to assess the compliance of transient processes with technological requirements [11].

All three indicators (30) to (32) are used for comparative quality assessment. The controller is synthesized by mini-

mizing the MPC functional (26), and not by the ITAE criterion. The ITAE indicator is applied only at the stage of comparing already synthesized controllers. It simultaneously penalizes the amplitude and duration of deviations; therefore, it most fully reflects requirements (1) to (3). It is for ITAE that the greatest advantage of MPC is recorded, therefore it is called the main criterion of comparison.

The dynamic characteristics of the system are additionally evaluated by time criteria, which reflect the quality of the transient process and the ability of the system to suppress disturbances.

Overshoot is defined as

$$\sigma = \frac{y_{\max - y_{sp}}}{y_{sp}} \cdot 100\%. \quad (33)$$

The settling time is defined as the interval during which the output variable enters and remains within the specified tolerance δ

Ts – time to settle to δ-band ($\delta = 2\%$). (34)

The efficiency of suppressing external disturbances is characterized by the coefficient

$$K_{dist} = \max \frac{\left| e_{dist}(t) \right|}{\Delta d}, \quad (35)$$

where Δd is the amplitude of the applied disturbance. A decrease in the K_{dist} value shows an increase in the robustness of the system and its ability to minimize the influence of external factors on the output variable [21].

5. 5. Determining effectiveness of the adaptive-predictive control system in MATLAB

Numerical modeling of the adaptive-predictive control system was performed in the MATLAB environment (USA) based on the discretization of the hydrodynamic model of the pipeline, described by equations (4) to (15) and the dynamic equation (12). The purpose of the simulation was to implement a single algorithm for the interaction of the hydrodynamic model, adaptive identification, and predictive controller in a closed control loop (Fig. 1).

The simulation was performed for 150 min and consisted of two stages: pressing (0–30 min) and operating mode (30–150 min). During the pressing stage, the pressure in the pipeline increased from atmospheric to the calculated operating level, reproducing the real procedure for starting main systems.

The initial uniform pressure distribution is given by the condition

$$P(x,0) = P_{atm} = 10^5 \text{ Pa}.$$

This condition corresponds to a filled pipeline without pressure drop along the route.

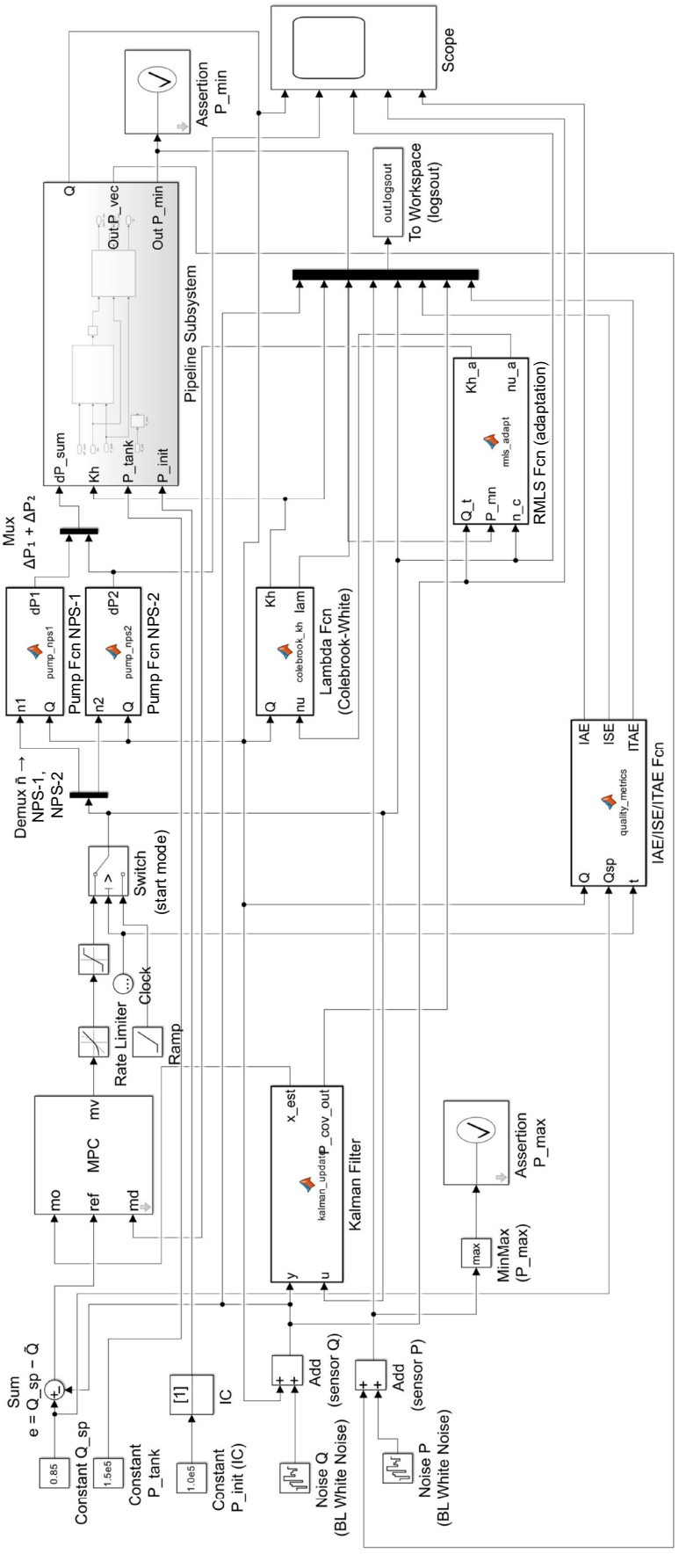

Fig. 1. Block diagram of the interaction algorithm of the hydrodynamic model, adaptive identification, and predictive controller in a closed control loop

After switching to the operating mode, a parametric disturbance is introduced in the form of a jump in oil viscosity. This scenario is used to check the operation of the adaptive circuit with changes in hydraulic resistance.

The calculation was performed at a step of $\Delta t = 2$ s and included the sequential execution of hydrodynamic calculation, state evaluation, and control synthesis. The hydraulic resistance coefficient K_h was updated at each step of the simulation, determined by local values of flow and viscosity using the Reynolds number and the Colebrook-White formula. The next step was to integrate the flow dynamics equation (12), and the spatial pressure distribution along the pipeline was determined by recursive integration from the boundary condition of the tank farm to the beginning of the route.

In our study, control system is a combination of the Kalman filter, recursive parameter identification, and MPC optimization. The Kalman filter performs state prediction using a discrete state space model with subsequent correction based on the measured flow rate, and as a result, this provides noise filtering and smoothed estimation. The model parameters are simultaneously refined using the recursive least squares method with a forgetting factor. All this made it possible to update the hydraulic coefficients in real time and compensate for changes in the properties of the medium.

The estimated state is used to form the MPC optimization problem, in which the deviation in the flow rate from the set value is minimized and the change in the control signals of the pumping stations is limited. The problem is solved on the forecast horizon, which shifts at each time step, taking into account the constraints on the pressure, flow rate, and rate of change in control influences. The resulting optimal values of the relative speed of rotation of the pumps are fed to the object, the cycle is repeated for the next step of modeling, which forms a closed control loop.

In the period of 0–30 min, both controllers worked according to the same law of pump acceleration from 0 to 0.9 p. u. By the time $t = 30$ min, the flow rate reached the value $Q_{sp} = 0.55$ m^3/s. After that, the difference between the algorithms became apparent. For MPC, the flow rate deviation did not exceed ±2% (±0.011 m^3/s). At $t = 60$ min, the viscosity increased from $4 \cdot 10^{-6}$ to $5.5 \cdot 10^{-6}$ m^2/s. Under this mode, the MPC maintained the flow rate near the setpoint, while the PID controller entered a long transient process with an exit beyond the permissible range.

The dynamics of pressures at the outlet of the pumping stations confirm the correctness of the implemented boundary conditions (Fig. 3). In the compression phase, the pressure at the outlet of NPS-1 increased from the atmospheric value (1 bar) in accordance with the linear increase in the speed of the pumps. The nominal level was reached in accordance with the characteristic $H = a_0 n^2 - a_1 Q^2$ at $n = 0.9$ and $Q = Q_{sp}$, which gives $\Delta P \approx 3.5$ MPa. The pressure at the outlet of NPS-2 did not exceed 37 bar, taking into account the residual backpressure after the first section of the route. No violation of the established limits was recorded during the entire simulation time.

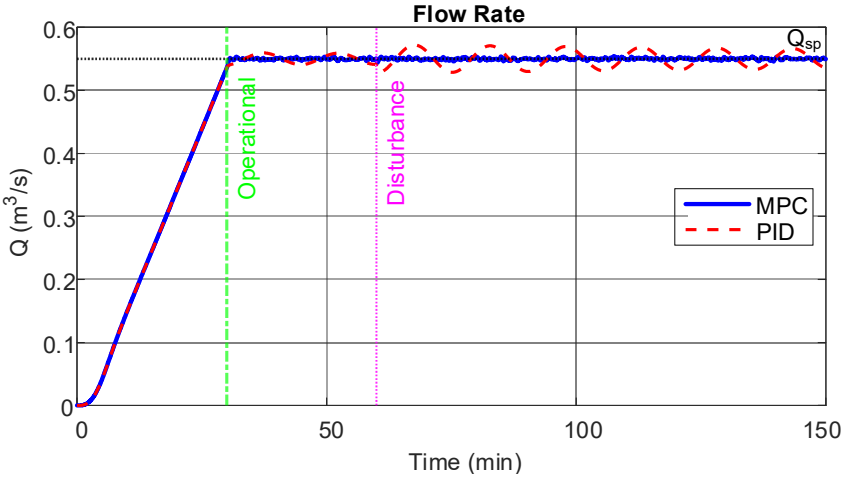

Fig. 2. Dynamics of oil flow in the pipeline $Q(t)$ for model-predictive and proportional-integrated-differential controllers

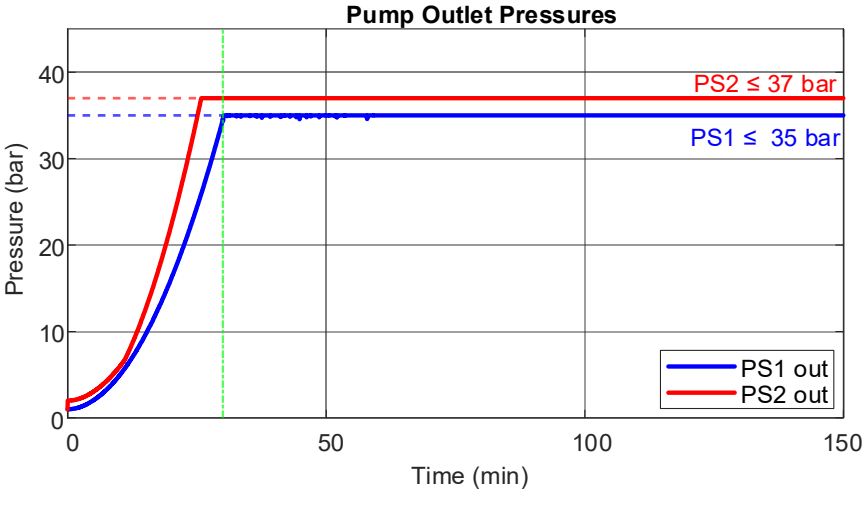

Fig. 3. Pressure at the outlet of the first and second pumping stations

Comparison of the pressures at the inlet and outlet of the pumping stations allowed us to assess the formation of local hydraulic differences (Fig. 4). The inlet pressure of NPS-1 is recorded at the atmospheric level ($P_{atm} = 1$ bar), since the station is powered from a reservoir with a small backpressure. The outlet pressure of NPS-1 was determined by the difference $\Delta P_1 = \mathrm{PS1_{out}} - P_{atm}$, which under the rated mode reached 34–35 bar. The inlet pressure at NPS-2 was formed by integration along the first section of the route (100 km), taking into account friction losses and the geodetic profile $z(x) = 20 \cdot \sin(\pi x / L) + 5 \cdot \sin(2\pi x / L)$ and under the steady state was 15–16 bar, which, at a margin, satisfies the requirement $\mathrm{PS2_{вх}} \geq 8$ bar. During the disturbance, the hydraulic resistance increased, the head at the inlet of NPS-2 decreased, and the controller compensated for this by increasing the pump speed within $n \leq 1.1$ p.u.

The integrated criterion of absolute error accumulated from the moment of transition to the operational phase (Fig. 5). Along the section of 30–60 min, the IAE curves of both controllers practically coincided. After the disturbance at $t = 60$ min, the increase in the indicator for the PID controller accelerated. The reason was the undamped fluctuations of the flow rate with periodic exits from the tolerance band. For MPC, the increase remained small due to the early compensation of the disturbance by the estimate $\hat{d}$.

The increase in ISE (31) during the operating phase was informative (Fig. 6). For the model-predictive controller with weighting coefficients $Q_w = 100$, $R_w = 50$, it turned out to be several times smaller than for the PID controller. This was explained by the fact that the flow rate did not exceed the tolerance band. Large instantaneous deviations, to which ISE is particularly sensitive, were absent.

The spatial distribution of pressure along the route reflected five characteristic moments in time (Fig. 7). The initial state corresponded to the atmospheric pressure along the entire route ($P = P_{atm} = 1$ bar). The profile was formed from the node $x = 0$ ($PS1_{out} \leq 35$ bar) with a monotonic decrease taking into account hydraulic losses and geodetic relief. At the node $x = 100$ km, the pressure received a second rise to a level ≤ 37 bar, after which it fell to $P_{tank} = 1.5$ bar in the tank farm. The minimum pressure at no node fell below $P_{min} = 2$ bar during the operation of the model-predictive controller, which confirmed the cavitation safety of the regime.

The estimate of the unmeasured disturbance $\hat{d}$ was formed by the Kalman filter. Its dynamics are shown in Fig. 8. Until the moment of disturbance, it was maintained at a constant level $\approx +1.1$ l/s. This level reflected the residual error of the linearization of the model (17) at the operating point. Immediately after the viscosity jump at $t = 60$ min, the estimate shifted to a new constant level ≈ -0.6 l/s within about one minute. The offset $\Delta\hat{d} \approx -1.7$ l/s was equivalent to the additional speed of the pumps. This speed was automatically introduced by the offset-free controller to compensate for the increased hydraulic resistance. It was this mechanism that enabled the processing of the parametric disturbance without the flow exceeding the tolerance limits.

The control error $e(t) = Q(t) - Q_{sp}$ (Fig. 9) clearly demonstrated the difference between the approaches. The MPC controller kept the flow rate deviation within ± 0.011 m^3/s (tolerance $\pm$ 2%) throughout the entire operating phase. This also applied to the moment of the viscosity jump at $t = 60$ min. Thanks to the compensation based on the disturbance $\hat{d}$ assessment, the short-term increase in the error did not go beyond the band. After the disturbance, the classical controller entered the mode of undamped oscillations with an amplitude of up to 15–20 l/s. At the same time, periodic deviations beyond the tolerance limits were observed due to the reactive correction principle.

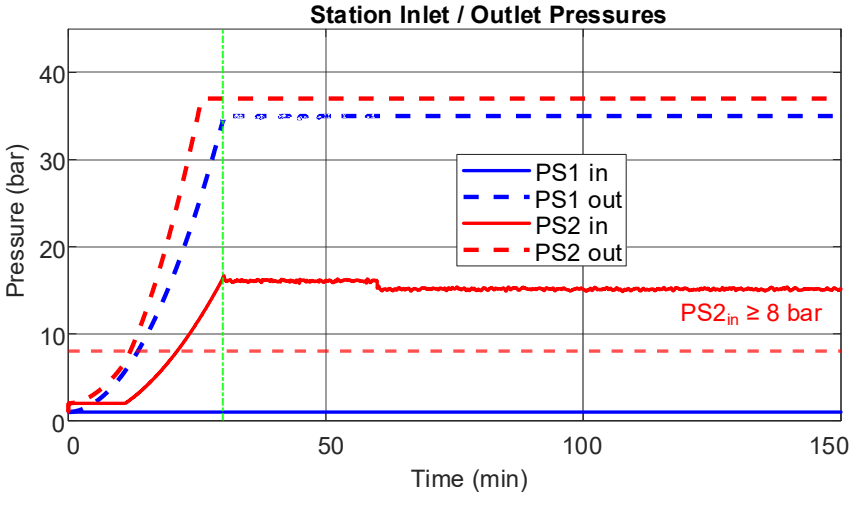

Fig. 4. Distribution of inlet and outlet pressure at pumping stations

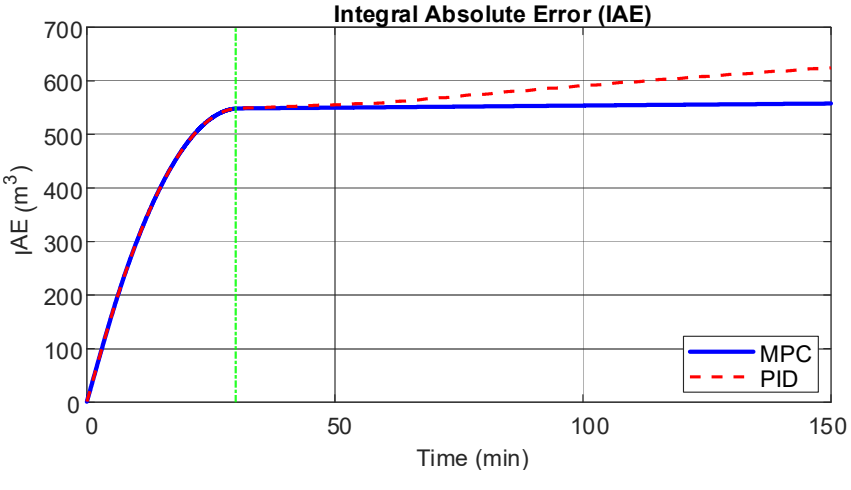

Fig. 5. Integrated absolute error of flow control

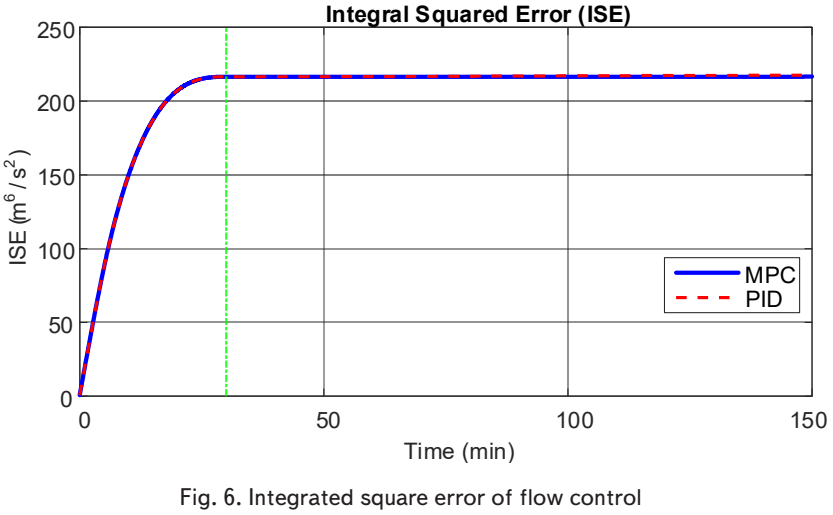

Fig. 6. Integrated square error of flow control

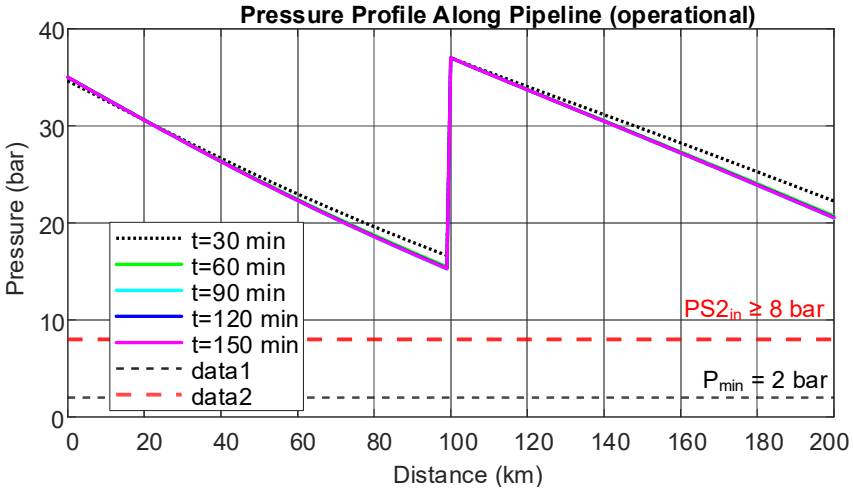

Fig. 7. Spatial pressure distribution along the pipeline

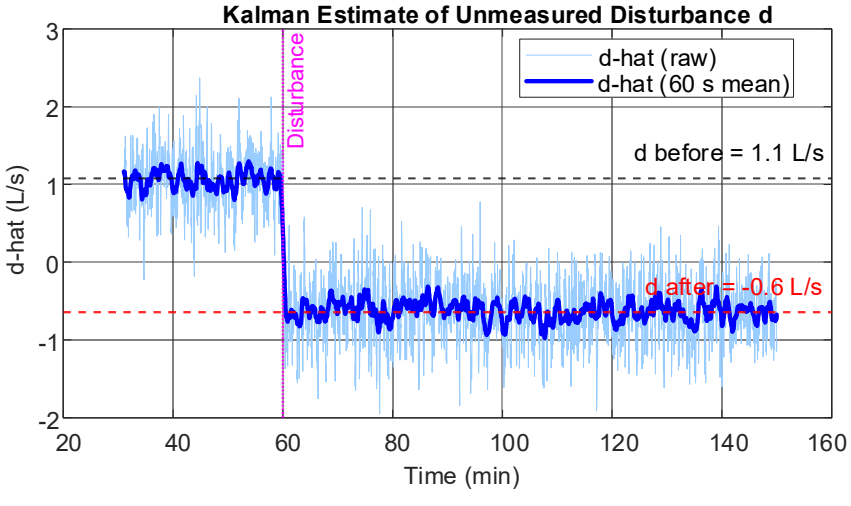

Fig. 8. Kalman filter estimation of unmeasured disturbance $\hat{d}$

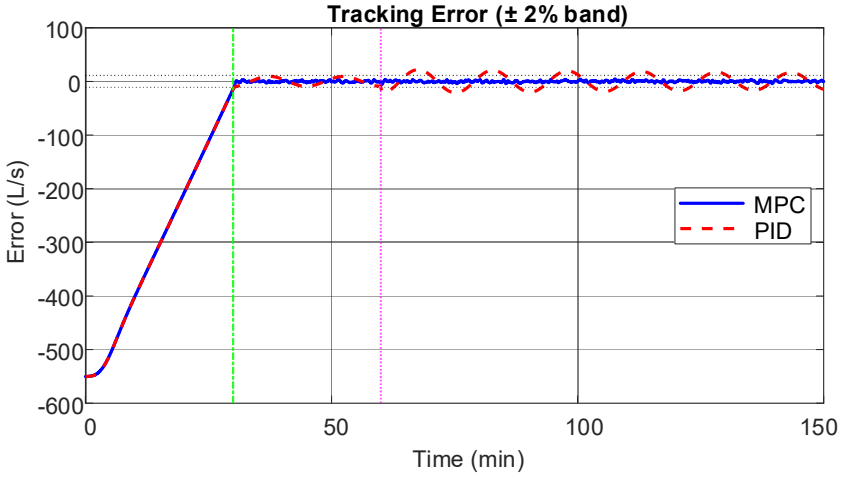

Fig. 9. Flow control error at a tolerance band of ±2%

The distribution of the minimum pressure along the route was considered as an important indicator of the cavitation stability of the system (Fig. 10). When the model-predictive controller was operating, the minimum pressure was reliably kept above the limit of $P_{\min}$ 2 bar throughout the entire simulation time.

After the disturbance, the amplitude of the flow rate deviations in the MPC circuit did not exceed 5 l/s, while in the PID control it reached 15–20 l/s (Fig. 9). A similar relationship was observed for the pressure: the range of minimum pressure fluctuations was about 0.4 bar for the MPC versus 2.6 bar for the PID controller (Fig. 10). At the same time, throughout the simulation, both controllers provided a minimum pressure significantly above the permissible level $P_{\min} = 2$ bar (and also $S2_{вх} \geq 8$ bar): the minimum value was

about 14 bar in the PID system and about 15.2 bar in the MPC system. After $t = 60$ min, undamped minimum pressure fluctuations with an amplitude of about ± 1.3 bar appeared in the PID controller circuit, while the MPC system entered a new steady-state mode with almost no oscillations. The difference is explained by the fact that the constraint $P_{\min} = 2$ bar is directly taken into account in the quadratic programming problem (27), therefore, throughout the entire simulation, it was performed at all pipeline nodes (Fig. 10).

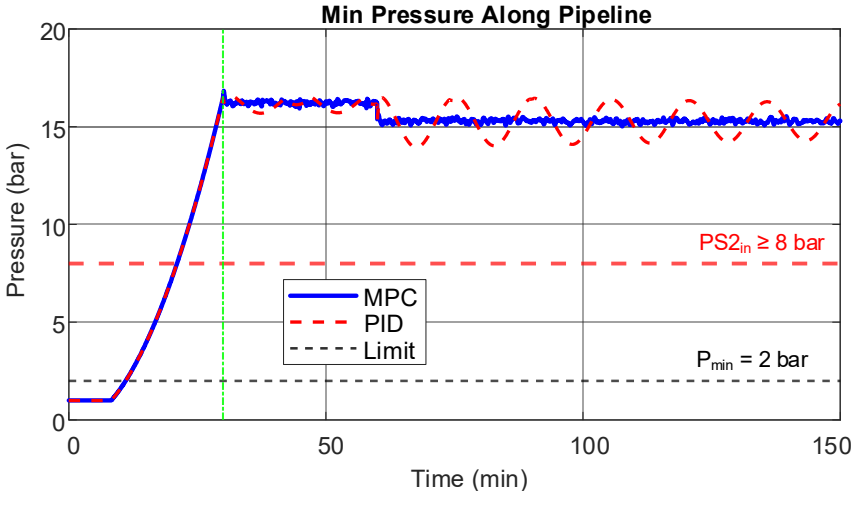

Fig. 10. Minimum pressure along the pipeline

The results by the integrated criterion also confirm the advantage of the proposed approach. The IAE increase during the operational phase was about 10 m^3 for the MPC versus 76 m^3 for the PID controller, i.e., it was almost eight times smaller. During the simulation, the flow rate in the MPC loop never left the ± 2% band (Fig. 9).

Regarding the operation of the identifier (Fig. 11): up to $t = 60$ min, the $\hat{d}$ estimate remained close to the true value of 0.8739, and the deviation did not exceed 0.05%. After a sudden change in viscosity, the estimate gradually shifted to a new value of 0.8682. Such dynamics are explained by the fact that in a stabilized loop the excitation level is small, and parameter updates are performed only if the signal is sufficiently informative.

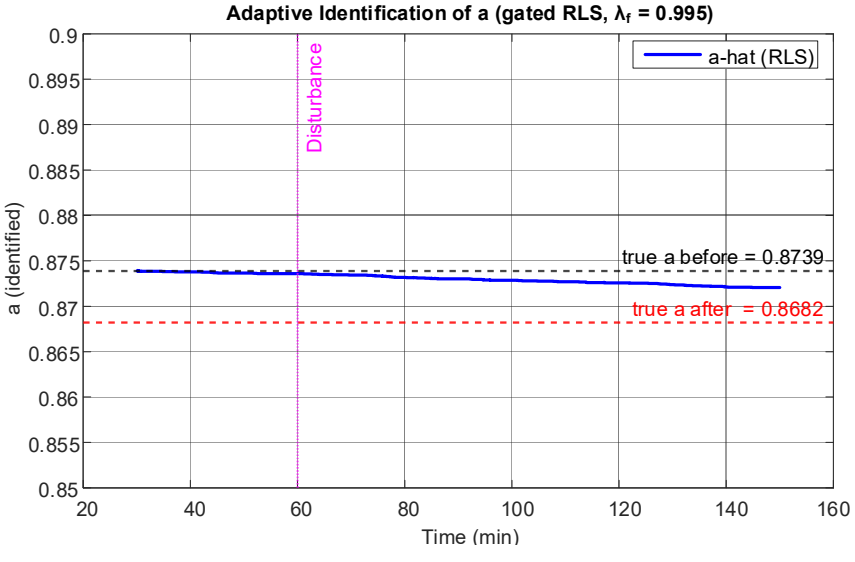

Fig. 11. Adaptive identification of dynamics parameter *a*

6. Discussion of results based on the synthesis of an adaptive-predictive system for controlling the hydrodynamic regimes in a main oil pipeline

The difference in the results is determined by the architecture of the controller itself. The PID algorithm is reactive in nature – the influence is formed on the basis of the already recorded error $e(t)$ according to (30). MPC, on the other hand, minimizes the predicted error on the horizon $Hp = 10$ steps according to (26), that is, it begins to correct the trajectory even before the disturbance fully manifests itself in the flow. Hence the fundamental difference: MPC keeps Q in the ± 2% band even at the moment of a viscosity jump, while PID enters an oscillatory mode with an amplitude of 3–4% of the setpoint (criteria (33) and (34)). The overall decrease in the IAE increase during the operational phase by approximately 87% (Fig. 5) is determined by two interrelated mechanisms.

The first mechanism is the state estimator. The Kalman filter (22) to (25) forms the extended state $\hat{x} = \left[\Delta\hat{Q}; d\right]^T$. The $\hat{d}$ estimate falls into the free term of the MPC forecast and therefore the disturbance is taken into account before its manifestation in the flow (offset-free structure [21]). A side effect is a significant suppression of measurement noise. The second mechanism is the parameter adapter (28), (29). When the viscosity jumps from $4 \cdot 10^{-6}$ to $5.5 \cdot 10^{-6}$ m^2/s, the recursive LSM with the forgetting factor λ_f tracks the change in K_h and updates the forecast model before the flow deviation reaches a critical level.

Compliance with the cavitation constraint $P_{\min} = 2$ bar (1) at all pipeline nodes (Fig. 10) is explained by the explicit inclusion of this constraint in the quadratic programming problem (27). The classical controller after $t = 60$ min demonstrated undamped oscillations of the minimum pressure with an amplitude of about ± 1.3 bar (Fig. 10). This was a direct consequence of the absence of a forecast mechanism. The most critical zone is the section of the geodesic rise of the route at $x \approx 80$ km, where the profile $z(x) = 20 \cdot \sin(\pi x / L) + 5 \cdot \sin(2\pi x / L)$ reaches a local maximum and forms a pressure minimum (Fig. 7).

The dynamics of pressures at the outlet of pumping stations (Fig. 3) confirm the correct implementation of the boundary conditions. During compression, the pressure increases from 1 bar to ≈ 3.5 MPa in accordance with the pump characteristic (11); the difference $\Delta P_1 = \mathrm{PS1_{out}} - P_{atm}$ at NPS-1 under nominal mode reaches 34–35 bar (Fig. 4). The inlet pressure of NPS-2 under a steady mode is 15–16 bar (Fig. 4), which satisfies the requirement $\mathrm{PS2_{in}} \geq 8$ bar with a margin.

Compared to known approaches to predictive control over pipeline systems, the proposed system has four fundamental differences.

The first is model adaptation. In [10], the advantages of MPC are shown but most implementations work with unchanged parameters. Here, the RMNC (28), (29) is built into the control loop: the K_h parameters are updated automatically without stopping and manual reconfiguration. A similar concept was considered in [13], but without taking into account the specifics of hydraulic objects with distributed parameters.

The second is coordination of several stations. In [12], unsteady hydraulics with restrictions are implemented, but the controller covers one station. Here, MPC simultaneously optimizes $\overline{n}_1$ and $\overline{n}_2$ for both stations. When pressing, both receive an identical linear signal according to law (14). In the operational phase, the predictive controller distributed speed corrections between stations symmetrically. Such coordination ensured the coordinated formation of the total head without overloading a separate station.

Third: in [14], schemes for taking into account delayed and irregular measurements in the extended Kalman filter were proposed and the advantages for chemical technological systems were shown. In our work, this approach was adapted to hydraulic objects with distributed parameters. The measurement vector included the flow rate (Fig. 2). The correction of the state estimation was implemented by equation (24). Compared with the results reported in [7], where Kalman filtering was applied to nonlinear systems in a general statement, in our work the estimation procedure was coordinated with the linearized hydrodynamic model (17) to (19).

Fourth: full operating cycle. Most studies, in particular [9, 11], consider only the operational mode. Here, the entire cycle is implemented: from pressing (0–30 min, equations (13) to (15)) to stable transportation. This makes it possible to use the state accumulated by the Kalman filter at startup to initialize the estimator in the operational phase.

Our results have certain application limits that should be known when using the system in practice.

The results should be considered taking into account the limitations of the proposed mathematical model. The hydrodynamic model is based on one-dimensional equations (4), (5) with a quasi-stationary approximation for the friction coefficient. This limits the adequacy of the description for fast hydraulic transients with time scales smaller than the acoustic wave propagation time $L / c \approx 200 \cdot 10^3 / 1200 \approx 167$ s. To analyze hydraulic shocks during emergency pump stops, it is necessary to use a full elastic shock model according to the approach given in [1].

The effectiveness of the adaptive identifier also depends on the range of parametric disturbances. The adaptive identifier (28) and (29) correctly tracks viscosity changes in the range $\nu \in [3 \cdot 10^{-6}; 8 \cdot 10^{-6}]$ m^2/s, which corresponds to the conditions for transporting light oil [4]. With more abrupt changes, typical for heavy oils with $\nu > 10^{-5}$ m^2/s, the convergence of the recursive identifier may slow down, which would require a decrease in the forgetting coefficient λ_f.

In addition, the quality of MPC operation is determined by the conditions of its application. The controller has been synthesized based on the linearized model (17) to (19) at the operating point $Q0 = 0.55$ m^3/s, $\overline{n}_0 = 0.9285$. With a significant deviation from this point, for example, at a flow rate near the limits of range (2), the K_{ob} and T_{ob} coefficients change, which could lead to a deterioration in the quality of control without additional relinearization.

Our results are based on numerical simulation in the MATLAB environment with deterministically specified measurement noises. Actual measurement systems at oil pumping stations may have uncalibrated offsets and non-stationary noise, which would require additional tuning of the Kalman filter covariance matrices Q_f and R_f (equation (23)).

An additional factor affecting the adaptation efficiency is the time characteristics of the algorithm. The effective memory window of the adapter is ≈ 200 discrete steps at $\lambda_f = 0.995$ (formula (29)); and the estimates are updated only at moments of sufficient excitation. With more frequent or sharp changes in parameters than one jump in 120 min ($t = 60$ min from the beginning of the operational phase), the slow identification channel may not have time to converge to the next disturbance; in this case, the compensation is taken by the fast channel – the Kalman filter estimation of disturbance $\hat{d}$.

Unlike the application limits, the following shortcomings are peculiarities of the current implementation and could be eliminated within the same approach.

The first drawback is the simplified implementation of the MPC optimization kernel in the form of a gradient step instead of a full-fledged solver of the quadratic programming problem (27). The approach provides computational efficiency but does not guarantee global optimality with several simultaneously active constraints. It is recommended to replace it with a proven QP solver (Quadratic Programming), implemented, for example, according to the approach described in [20], which provides guaranteed optimality at acceptable computational costs on an industrial controller.

The second drawback is the uniform grid with a step of $\Delta x = 1$ km in equation (9). Near geodetic differences ($x \approx 80$ km) and pumping stations, the accuracy of P_i calculation may be insufficient. Solution: non-uniform grid or finite element method according to [3].

The third drawback is the lack of verification of the model on real industrial data from an oil pipeline. The coefficients $a_0 = 554.5$ m and $a_1 = 200$ m·s^2/m^{2}m^6 in equation (11) are taken from specifications for the NM 3600-230 pumps, and not from identification by real measurements. Verification should be performed using SCADA data on the real oil pipeline checking indicators (31) to (35).

The fourth drawback is the lack of explicit consideration of wear and tear of the pumping equipment. The characteristic $H = a_0 n^2 - a_1 Q^2$, embedded in equation (10), is considered to be invariant in time, while the real pump head degrades with operation. Elimination: introduction into the parameter vector θ (formula (28)) of an additional degradation parameter, which is tracked by the RMNK identifier.

Further advancement of our study should involve a transition from linear MPC to nonlinear predictive control based on the full nonlinear hydrodynamic model (4) to (12). This would allow us to correctly take into account the nonlinear dependence of the friction coefficient on the flow rate according to the Colebrook–White formula (6) over a wide range of modes. The theoretical basis of such an approach is embedded in [13]; however, its implementation requires solving the problem of nonlinear programming in real time, which is much more computationally complex than the current implementation (27).

The proposed control system employs a linearized pipeline model. Therefore, beyond the scope of our work is the study on nonlinear MPC based on the full model (4) to (12), in which the friction coefficient λ is determined directly from the Colebrook–White equation (6). Such an approach could allow us to abandon local linearization but would require solving the nonlinear optimization problem in real time [13], which is much more complex than the current algorithm (27).

The state estimation was performed using a linear Kalman filter. For regimes with significant deviations from the operating point, it is advisable to investigate the use of an extended Kalman filter [7]. In this case, it is necessary to separately evaluate the impact of linearization errors on the quality of the estimation and the stability of the algorithm, and this will also require larger computational resources and additional tuning of the linearization error matrices.

Our paper does not consider the use of hybrid models that combine the physical description of the process by equations (4) to (12) with neural network approximation methods [18]. This approach could be useful for compensating for errors in a simplified pipeline model but requires industrial data for training and validating the model [19].

Another area of further research is the application of the proposed controller in a multi-level control system. In this case, the upper level plans the daily flow regime, the lower one implements the operational MPC control designed in our work. This approach could make it possible to simultaneously solve the tasks of energy efficiency and technological safety, which is most often encountered in systems with a variable daily pumping schedule.

7. Conclusions

1. A mathematical notation for hydrodynamic processes along a section in a conditional oil pipeline has been constructed, which takes into account the variability of the environment parameters and the uncertainty in hydraulic characteristics. Unlike classical stationary models, the approach considers the dependence of hydraulic resistance on the oil flow regime. The model is a verification tool for studying the control method and does not claim to reproduce actual industrial conditions. The practical significance of the model is the trouble-free development of control algorithms before industrial implementation. This reduces the costs of setting up oil pipeline automation systems.

2. An adaptive-predictive controller has been synthesized, which implements optimal control on a finite horizon taking into account the constraints on pressure, flow rate, and dynamics of control influences. Unlike PID controllers, control is formed on the basis of a forecast of the future behavior of the system. This makes it possible to prevent violations of constraints before they occur. The stabilization effect is explained by the explicit consideration of the dynamics of the object and the estimation of the disturbance in the optimization problem.

3. The problem of state estimation and recursive identification of parameters of a hydrodynamic system under conditions of measurement noise has been solved. The solution combines the Kalman filter with an extended state vector and a scalar RMNK with a forgetting coefficient and an excitation threshold. The state and parameter estimation is performed consistently in real time, without assuming model constancy. Noise filtering improves the quality of identification while updated parameters reduce model uncertainty of the estimation.

4. An intelligent control support component based on the Kalman filter with an extended state vector has been designed. It combines the estimation of an unmeasured disturbance with a scalar recursive identification of the dynamics parameter. The disturbance estimation responded to a viscosity jump within approximately one minute. The identified dynamics parameter reproduced the true value with an error of less than 0.05% before the disturbance. The difference from classical schemes is the decomposition of adaptation into a fast channel (disturbance $\hat{d}$) and a slow channel (parameter a). This eliminates the bias of estimates and the growth of covariance in the steady state.

5. A software implementation and numerical study of an integrated control system in the MATLAB environment covering the full cycle of operation of the main oil pipeline from start-up modes to stationary operation have been performed. The simulation results showed a decrease in the IAE increase during the operational phase by approximately 87% (≈ 10 m^3 versus ≈ 76 m^3 in PID); maintaining the flow rate within the technological tolerance of $\pm 2\%$ over the entire operational phase, including the moment of viscosity jump; as well as guaranteed compliance with pressure restrictions ($P_{\min} = 2$ bar, $PS2_{in} \geq 8$ bar) during the operation of MPC controller. The practical significance is as follows: the proposed algorithm has been implemented as a discrete closed-loop system with a step of 2 s and could be integrated into a SCADA controller at an oil pumping station. This would provide automatic compensation for changes in oil viscosity without stopping and reconfiguring the system, increase energy efficiency, and reduce cyclic loads on equipment. The achieved effect is explained by the closed structure of the system, in which the interaction of identification, condition assessment, and predictive optimization enables self-adjustment to current operating conditions.

Conflicts of interest

The authors declare that they have no conflicts of interest in relation to the current study, including financial, personal, authorship, or any other, that could affect the study and the results reported in this paper.

Funding

The study was conducted without financial support.

Data availability

All data are available in the main text of the manuscript.

Use of artificial intelligence

In the process of conducting the research, artificial intelligence tools were used as auxiliary toolset at the stage of development and verification of the software implementation of the proposed algorithms. In particular, to check the correctness of the code of the hydraulic system model and adaptive-predictive control algorithms in the MATLAB environment, a chatbot based on the large language model Claude Sonnet 4.6 (Anthropic, USA), version of the first half of 2026, was used, as well as for linguistic-stylistic editing of the manuscript. The share of text with the participation of AI is no more than 25%.

The AI assistant was involved in analyzing the structure of the program code, identifying potential implementation

errors, coordinating numerical procedures with the mathematical statement of the problem, as well as to check the compliance of the algorithmic implementation with the theoretical provisions set out in the work. Special attention was paid to assessing the stability of computational procedures and the correctness of the implementation of recursive algorithms in discrete time.

The numerical results were obtained by the authors on their own resource. AI did not have access to the input data and did not generate the results. Scientific evidence, conclusions, and interpretation are the expert work of the authors. The use of AI did not affect the novelty, reliability, or reproducibility of the results.

Authors' contributions

Oleksandr Kuchmystenko: Methodology, Software, Formal analysis, Investigation, Writing – original draft; **Mykhailo Shavranskyi:** Software, Validation, Investigation; **Yurii Puk:** Investigation, Formal analysis, Writing – review & editing.

References

1. Chaudhry, M. H. (2014). Applied Hydraulic Transients. Springer New York. https://doi.org/10.1007/978-1-4614-8538-4
2. Zeghadnia, L., Robert, J. L., Achour, B. (2019). Explicit solutions for turbulent flow friction factor: A review, assessment and approaches classification. Ain Shams Engineering Journal, 10 (1), 243–252. https://doi.org/10.1016/j.asej.2018.10.007
3. Tentis, E., Margaris, D., Papanikas, D. (2003). Transient gas flow simulation using an Adaptive Method of Lines. Comptes Rendus. Mécanique, 331 (7), 481–487. https://doi.org/10.1016/s1631-0721(03)00106-2
4. Muñoz, J. A. D., Ancheyta, J., Castañeda, L. C. (2016). Required Viscosity Values To Ensure Proper Transportation of Crude Oil by Pipeline. Energy & Fuels, 30 (11), 8850–8854. https://doi.org/10.1021/acs.energyfuels.6b01908
5. Azizi, N., Homayoon, R., Hojjati, M. R. (2018). Predicting the Colebrook–White Friction Factor in the Pipe Flow by New Explicit Correlations. Journal of Fluids Engineering, 141 (5). https://doi.org/10.1115/1.4041232
6. Simon, D. (2006). Optimal State Estimation. Wiley. https://doi.org/10.1002/0470045345
7. Simon, D. (2010). Kalman filtering with state constraints: a survey of linear and nonlinear algorithms. IET Control Theory & Applications, 4 (8), 1303–1318. https://doi.org/10.1049/iet-cta.2009.0032
8. Borase, R. P., Maghade, D. K., Sondkar, S. Y., Pawar, S. N. (2020). A review of PID control, tuning methods and applications. International Journal of Dynamics and Control, 9 (2), 818–827. https://doi.org/10.1007/s40435-020-00665-4
9. Wang, L. (2004). A Tutorial on Model Predictive Control: Using a Linear Velocity-Form Model. Developments in Chemical Engineering and Mineral Processing, 12 (5-6), 573–614. https://doi.org/10.1002/apj.5500120511
10. Qin, S. J., Badgwell, T. A. (2003). A survey of industrial model predictive control technology. Control Engineering Practice, 11 (7), 733–764. https://doi.org/10.1016/s0967-0661(02)00186-7
11. Mayne, D. Q., Rawlings, J. B., Rao, C. V., Scokaert, P. O. M. (2000). Constrained model predictive control: Stability and optimality. Automatica, 36 (6), 789–814. https://doi.org/10.1016/s0005-1098(99)00214-9
12. Zeng, W., Wang, C., Yang, J. (2022). Hydraulic Transient Simulation of Pipeline-Open Channel Coupling Systems and Its Applications in Hydropower Stations. Water, 14 (18), 2897. https://doi.org/10.3390/w14182897
13. Allgöwer, F., Zheng, A. (Eds.) (2000). Nonlinear Model Predictive Control. Birkhäuser Basel. https://doi.org/10.1007/978-3-0348-8407-5
14. Gopalakrishnan, A., Kaisare, N. S., Narasimhan, S. (2011). Incorporating delayed and infrequent measurements in Extended Kalman Filter based nonlinear state estimation. Journal of Process Control, 21 (1), 119–129. https://doi.org/10.1016/j.jprocont.2010.10.013
15. Ljung, L. (1998). System Identification. Signal Analysis and Prediction, 163–173. https://doi.org/10.1007/978-1-4612-1768-8_11
16. Ioannou, P., Fidan, B. (2006). Adaptive Control Tutorial. SIAM. https://doi.org/10.1137/1.9780898718652
17. Gülich, J. F. (2014). Centrifugal Pumps. Springer Berlin Heidelberg. https://doi.org/10.1007/978-3-642-40114-5
18. Bikmukhametov, T., Jäschke, J. (2020). Combining machine learning and process engineering physics towards enhanced accuracy and explainability of data-driven models. Computers & Chemical Engineering, 138, 106834. https://doi.org/10.1016/j.compchemeng.2020.106834
19. Nelles, O. (2001). Nonlinear System Identification. Springer Berlin Heidelberg. https://doi.org/10.1007/978-3-662-04323-3
20. Camacho, E. F., Bordons, C. (2007). Model Predictive control. Springer London. https://doi.org/10.1007/978-0-85729-398-5
21. Pannocchia, G., Rawlings, J. B. (2003). Disturbance models for offset-free model-predictive control. AIChE Journal, 49 (2), 426–437. https://doi.org/10.1002/aic.690490213